a value of 116 ppm was found for (OEP)Rh(μ-CO)RhOEP (OEP = octaethylporphyrin ligand).[20] Thus, such a dimetallo ketone bridging CO ligand requires σ bonds between the metals and the carbon atom so that the oxidation state of iridium is formally +III.

Stability of Complex 2a. The two complexes **2a** and **2b** are thermally resistant. Indeed after a week in boiling benzene only half of the complexes were converted into the complexes **3a** and **3b** by loss of a CO ligand. The reverse addition of CO to **3a** was not observed under the ambient conditions since no traces of **2a** were detected by infrared. Moreover, addition of Me_3NO to assist the decarbonylation of complex **2a** increased the CO loss only slightly even in boiling benzene. However we noted that exposure of complex **2a** to natural light in solution or even in the solid state gives rise to a very fast extrusion of the bridging CO ligand to form complex **3a**. Irradiation of solutions with sunlight is a good way to obtain **3a** from **2a** in a few minutes.

Mechanism of the Formation of 2a and 2b. Clearly, the formation of the μ-CO ligand in the complexes under interest is due to the fast attack of iodine to an intermediate species formed after the addition of phosphine. Indeed the addition of iodine to $Ir_2(\mu\text{-S-}t\text{-Bu})_2(CO)_4$ to give $Ir_2(\mu\text{-S-}t\text{-Bu})_2(CO)_4I_2$ and to $Ir_2(\mu\text{-S-}t\text{-Bu})_2(CO)_2L_2$ giving $Ir_2(\mu\text{-S-}t\text{-Bu})_2(CO)_2L_2I_2$ was shown to proceed very quickly. In this study, these two complexes were not detected by infrared even at the beginning of the reaction. Complex $(CO)_2(PMe_3)(S\text{-}t\text{-Bu})Ir(\mu\text{-S-}t\text{-Bu})Ir(CO)_2(PMe_3)$ (**5**) was previously proposed as an intermediate to explain the formation of two intermediate species characterized by X-ray, $Ir_2(\mu\text{-S-}t\text{-Bu})(\mu\text{-CO})(CO)_2(PMe_3)_2(S\text{-}t\text{-Bu})$ and $Ir_3(\mu\text{-S-}t\text{-Bu})_3(\mu\text{-CO})(CO)_4(PMe_3)_2$, when 2 equiv of trimethylphosphine are added to **1**.[21] The attack of iodine on complex **5** is believed to proceed very fast and through a radical process, as initially shown by Osborn on mononuclear complexes[22] and proposed for the formation of complexes **3**.[13] Presumably a first attack of iodine on a single iridium atom of **5** occurs to give I$^\bullet$ and $[(CO)_2(PMe_3)(S\text{-}t\text{-Bu})Ir(\mu\text{-S-}t\text{-Bu})Ir(CO)_2(PMe_3)I]^\bullet$ (**6**), a d^8–d^7 species. Very recently Stobart et al. have shown that a d^8–d^7 complex could be isolated resulting from the oxidative addition of iodine to the complex $Ir_2(\mu\text{-pyrazolato})_2(1,5\text{-}C_8H_{12})_2$.[23] We suggest that in this species **6** an internal attack of a carbonyl ligand coordinated to the d^7 iridium atom on the Ir(I) atom, with simultaneous loss of a terminal CO ligand, gives rise to the d^7–d^6 species **7**, $[(CO)(PMe_3)(S\text{-}t\text{-Bu})Ir(\mu\text{-S-}t\text{-Bu})(\mu\text{-CO})Ir(CO)(PMe_3)I]^\bullet$. Finally a second radical process of **7** with I$^\bullet$ or with I_2 generates complex **2**.

Acknowledgment. ATOCHEM Co. is gratefully acknowledged for financial support and for a grant to J.F. We also thank the CNRS through the operation "GRECO Oxydes de Carbone" and the "Ministerio de Education y Ciencia" of Spain for a grant to C.C. We are indebted to Dr. J. Galy (Giter-CNRS) for helpful discussions.

Registry No. **1**, 63312-27-6; **2a**, 109839-53-4; **2b**, 109839-52-3.

Supplementary Material Available: Listings of anisotropic general temperature factors, root-mean-square amplitudes of thermal vibrations, least-squares planes, bond angles, and hydrogen atom positional and isotropic thermal parameters (9 pages); a listing of calculated and observed structure factors (22 pages). Ordering information is given on any current masthead page.

---

[19] Mann, B. E.; Taylor, B. B. *^{13}C NMR Data for Organometallic Compounds*; Academic: New York, 1981; Table 2.8.

[20] Wayland, B. B.; Woods, B. A. ;Coffin U. L. *Organometallics* **1986**, *5*, 1059.

[21] Kalck, P.; Bonnet, J. J. ; Poilblanc, R. *J. Am. Chem. Soc.* **1982**, *104*, 3069.

[22] Bradley, J. S.; Connor, D. E.; Osborn, J. A. *J. Am. Chem. Soc.* **1972**, *94*, 4043.

[23] Fjeldsted, D. O. X.; Stobart, S. P.; Zaworotko, M. G. *J. Am. Chem. Soc.* **1985**, *107*, 8258. Harrison, D. G.; Stobart, S. R. *J. Chem. Soc., Chem. Commun.* **1986**, 285.

Contribution from the Departamento de Quimica Inorganica, Instituto de Ciencia de Materiales de Aragon,
Universidad de Zaragoza—CSIC, 50009 Zaragoza, Spain, and Department of Chemistry
and Laboratory for Molecular Structure and Bonding, Texas A&M University, College Station, Texas 77843

Heterotrinuclear Pt_2Ag Clusters with Pt–Ag Bonds Unsupported by Covalent Bridges. Molecular Structures of $(NBu_4)_2[Pt_2(\mu\text{-}Cl)_2(C_6F_5)_4]$ and $(NBu_4)[Pt_2AgCl_2(C_6F_5)_4O(C_2H_5)_2]$

Rafael Uson,*[†] Juan Fornies,[†] Milagros Tomas,[†] Jose M. Casas,[†] F. Albert Cotton,*[‡] and L. R. Falvello[‡]

Received May 13, 1987

The preparation and properties of new trinuclear (Pt_2Ag) clusters are reported. The compounds $(NBu_4)[Pt_2AgX_2(C_6F_5)_4OEt_2]$ (X = Cl (**1**), Br (**2**)) are formed by reaction of $(NBu_4)_2[Pt_2(\mu\text{-}X)_2(C_6F_5)_4]$ with $AgClO_4$ in dichloromethane/diethyl ether solution. The phosphine-substituted products $(NBu_4)[Pt_2Ag(\mu\text{-}Cl)_2(C_6F_5)_4L]$ (L = PPh_3 (**3**), $PMePh_2$ (**4**)) are formed by the reaction of $(NBu_4)_2[Pt_2(\mu\text{-}Cl)_2(C_6F_5)_4]$ with $AgOClO_3L$ at −30 °C. Product **3** is also formed by the reaction of **1** with PPh_3 in dichloromethane at −30 °C. The products were characterized by elemental analysis, conductance measurements, and IR spectroscopy. The precursor $(NBu_4)_2[Pt_2(\mu\text{-}Cl)_2(C_6F_5)_4]$ and product **1**, $(NBu_4)[Pt_2Ag(\mu\text{-}Cl)_2(C_6F_5)_4OEt_2]$, were analyzed by X-ray diffraction. Crystals of $(NBu_4)_2[Pt_2(\mu\text{-}Cl)_2(C_6F_5)_4]$ are monoclinic, space group $P2_1/c$, with $a = 12.763$ (4) Å, $b = 12.858$ (4) Å, $c = 19.554$ (7) Å, $\beta = 104.62$ (2)°, $V = 3105$ (2) Å^3, and $Z = 2$. The structure was refined to residuals of $R = 0.0399$, $R_w = 0.0525$, and quality-of-fit = 1.044, with 370 parameters and 2960 data. The $Pt_2Cl_2C_4$ core of the complex anion is planar. Crystals of product **1** are monoclinic, space group $P2_1/n$, with $a = 12.574$ (2) Å, $b = 14.749$ (2) Å, $c = 27.983$ (3) Å, $\beta = 92.73$ (1)°, $V = 5184$ (2) Å^3, and $Z = 4$. The structure was refined to final residuals of $R = 0.0397$, $R_w = 0.0448$, and quality-of-fit = 1.088, with 640 parameters and 4252 observations. While there is no direct Pt–Pt bond in **1**, the two Pt–Ag bonds are unbridged and have bond lengths of 2.782 (1) and 2.759 (1) Å. There are no close contacts between the silver atom and the fluorine atoms of the C_6F_5 ligands.

Introduction

For several years we have been studying the reactions between anionic (perhalophenyl)platinum(II) complexes, which behave as nucleophiles because of their negative charges, and suitable silver salts ($AgClO_4$, $AgNO_3$, or $R_3PAgOClO_3$), which serve as the electrophilic complements, although they can also act as halide abstractors. To date, we have observed and reported the following results.

1. An anionic Pt complex that contains no halide ligand ($[Pt(C_6F_5)_3(SC_4H_8)]^-$) reacts with a silver salt (eq 1) to give a

$$(NBu_4)[Pt(C_6F_5)_3(SC_4H_8)] + O_3ClOAgP(C_6H_5)_3 \xrightarrow{CH_2Cl_2} NBu_4ClO_4 + [(SC_4H_8)(C_6F_5)_3PtAgP(C_6H_5)_3] \quad (1)$$

neutral binuclear complex with an unbridged Pt–Ag bond of length

---

[†] Universidad de Zaragoza—CSIC.

[‡] Texas A&M University.

0020-1669/87/1326-3482$01.50/0

Table I. Analytical[a] and Conductivity Data[b]

	anal., % C	anal., % H	anal., % N	Λ_M, Ω^{-1} cm^2 mol^{-1}
$(NBu_4)[Pt_2AgCl_2(C_6F_5)_4OEt_2]$ (**1**)	34.33 (33.91)	3.07 (2.96)	0.74 (0.90)	105
$(NBu_4)[Pt_2AgBr_2(C_6F_5)_4OEt_2]$ (**2**)	32.02 (32.17)	2.70 (2.80)	1.13 (0.85)	113
$(NBu_4)[Pt_2AgCl_2(C_6F_5)_4PPh_3]$ (**3**)	40.60 (39.99)	3.00 (2.92)	1.12 (0.80)	90
$(NBu_4)[Pt_2AgCl_2(C_6F_5)_4PMePh_2]$ (**4**)	37.46 (37.89)	2.99 (2.92)	1.10 (0.83)	100

[a] Calculated values in parentheses. [b] In acetone at ca. 20 °C.

2.637 (1) Å — shorter than any previously observed Pt–Ag bond.[1]

2. If the starting Pt complex contains both halide and perhaloaryl ligands, then although halide abstraction by silver can take place, the use of an excess of the silver salt leads to the formation of a trinuclear Pt_2Ag cluster[1a] (eq 2).

$$2(NBu_4)_2[Pt(C_6F_5)_3Cl] \xrightarrow[(C_2H_5)_2O]{AgClO_4,\ CH_2Cl_2} 2AgCl + 3(NBu_4)ClO_4 + (NBu_4)[Pt_2Ag(C_6F_5)_6(C_2H_5)_2O]\cdot O(C_2H_5)_2 \qquad (2)$$

For the cases described by eq 1 and 2, the analogous platinum-containing starting materials with C_6Cl_5 rather than C_6F_5 ligands have not yet been prepared. Thus, we have not yet determined what influence the nature of the perhaloaryl ligand has upon the results obtained. However, the anionic starting complexes $[\textit{trans}\text{-}PtCl_2(C_6X_5)_2]^{2-}$ (X = F,[2] Cl[3]) are both known, and so we have studied the reactions of both with $AgClO_4$. In neither case has any halide abstraction been observed. The products obtained in the two cases are substantially different from each other.

3. The complex $(NBu_4)_2[\textit{trans}\text{-}PtCl_2(C_6F_5)_2]$ reacts with $AgNO_3$ or $AgClO_4$ according to eq 3 to give[4] an anionic tetranuclear cluster containing both Pt–Ag bonds and Pt–Cl–Ag bridges.

$$2(NBu_4)_2[\textit{trans}\text{-}PtCl_2(C_6F_5)_2] + 2AgNO_3 \rightarrow 2(NBu_4)NO_3 + (NBu_4)_2[Pt_2Ag_2Cl_4(C_6F_5)_4] \qquad (3)$$

4. When the pentafluorophenyl ligands in the starting material of (3) are replaced by pentachlorophenyl groups, the result is different. Again, no AgCl precipitation is observed, but the product in this case[5] is the species $(NBu_4)_x[Pt(C_6Cl_5)_2(\mu\text{-}Cl)_2Ag]_x$, in which the anionic polymer has Pt–Cl–Ag bridges but no direct Pt–Ag bond.

A common and distinctive feature of all of these new complexes is the presence of short, nonbonding contacts between the silver atoms and *o*-halide atoms of the C_6X_5 groups. These contacts facilitate attractive forces that contribute to the stability of the clusters.

In this paper we report the extension of this work to the use of other Pt-containing starting materials, particularly the binuclear anionic complex $[Pt_2(\mu\text{-}X)_2(C_6F_5)_4]^{2-}$ (X = Cl, Br). This complex reacts with $AgClO_4$ or $O_3ClOAgL$ to form trinuclear Pt_2Ag clusters that have two unbridged Pt–Ag bonds and no Ag–*o*-F interaction.

Results and Discussion

Table II. Relevant IR Data (Frequencies in cm^{-1})

	X-sensitive	ν(Pt–Cl)
$(NBu_4)_2[Pt_2(\mu\text{-}Cl)_2(C_6F_5)_4]$	809 (vs) 798 (vs)	290 (m)
$(NBu_4)_2[Pt_2AgCl_2(C_6F_5)_4OEt_2]$ (**1**)	809 (vs) 801 (vs)	263 (m)
$(NBu_4)_2[Pt_2AgBr_2(C_6F_5)_4OEt_2]$ (**2**)	809 (vs) 800 (vs)	
$(NBu_4)_2[Pt_2AgCl_2(C_6F_5)_4PPh_3]$ (**3**)	809 (vs) 800 (vs)	262 (m)
$(NBu_4)_2[Pt_2AgCl_2(C_6F_5)_4PMePh_2]$ (**4**)	809 (vs) 799 (vs)	261 (w)

When a dichloromethane solution of equimolar amounts of $(NBu_4)_2[Pt_2(\mu\text{-}X)_2(C_6F_5)_4]$ (X = Cl, Br)[2] and $AgClO_4$ is stirred at room temperature for 3 h, no precipitate of AgX is formed. However, the complex $(NBu_4)[Pt_2AgX_2(C_6F_5)_4O(C_2H_5)_2]$ is formed, according to eq 4. The product can be isolated after the NBu_4ClO_4 has been removed by extraction with diethyl ether. (See the Experimental Section for details.)

$$(NBu_4)_2[Pt_2(\mu\text{-}X)_2(C_6F_5)_4] + AgClO_4 \xrightarrow{CH_2Cl_2/(C_2H_5)_2O} NBu_4ClO_4 + (NBu_4)[Pt_2AgX_2(C_6F_5)_4O(C_2H_5)_2] \qquad (4)$$

$$X = Cl\ (\mathbf{1}),\ Br\ (\mathbf{2})$$

Complexes **1** (X = Cl) and **2** (X = Br) both contain 1 equiv of diethyl ether coordinated to the silver atom. Both products are light sensitive but are otherwise stable at room temperature, both in the solid state and in solution.

The nature of the solvent used is important to the outcome of the reaction. If tetrahydrofuran is used, the product is the neutral mononuclear complex $[Pt(C_6F_5)_2(OC_4H_8)_2]$.[6]

Both of the products (with Cl or Br bridges) are obtained as oily residues upon evaporation of CH_2Cl_2 solutions. Extraction of the residue with diethyl ether (the NBu_4ClO_4 is insoluble), followed by filtration and evaporation of the extract, results in isolation of the trinuclear cluster compound with one OEt_2 molecule coordinated to silver in each case. The analytical data and ^1H NMR spectra are consistent with the formulations in the two cases.

It is possible to prepare, by two different routes, products in which phosphines rather than OEt_2 are coordinated to the silver atoms.

(a) Complex **1** reacts with an equimolar amount of PPh_3 in CH_2Cl_2 solution at −30 °C, to give $(NBu_4)[Pt_2Ag(\mu\text{-}Cl)_2(C_6F_5)_4PPh_3]$ (**3**) (eq 5).

$$(NBu_4)[Pt_2Ag(\mu\text{-}Cl)_2(C_6F_5)_4OEt_2] + PPh_3 \rightarrow (NBu_4)[Pt_2Ag(\mu\text{-}Cl)_2(C_6F_5)_4PPh_3] + OEt_2 \qquad (5)$$

(b) The starting material $(NBu_4)_2[Pt_2(\mu\text{-}Cl)_2(C_6F_5)_4]$ reacts with $AgOClO_3L$ (eq 6) to give the trinuclear complexes $(NBu_4)[Pt_2Ag(\mu\text{-}Cl)_2(C_6F_5)_4L]$ (L = PPh_3 (**3**), $PMePh_2$ (**4**)).

$$(NBu_4)_2[Pt_2(\mu\text{-}Cl)_2(C_6F_5)_4] + AgOClO_3L \xrightarrow[-30\ ^\circ C]{CH_2Cl_2} NBu_4ClO_4 + (NBu_4)[Pt_2Ag(\mu\text{-}Cl)_2(C_6F_5)_4L] \qquad (6)$$

Both of these processes require low temperature (−30 °C). At room temperature the phosphines cleave the bridges, and AgCl precipitates in all cases.

---

(1) (a) Uson, R.; Fornies, J.; Tomas, M.; Casas, J. M.; Cotton, F. A.; Falvello, L. R. *J. Am. Chem. Soc.* **1985**, *107*, 2556. (b) Cotton, F. A.; Falvello, L. R.; Uson, R.; Fornies, J.; Tomas, M.; Casas, J. M.; Ara, I. *Inorg. Chem.* **1987**, *26*, 1366.

(2) Uson, R.; Fornies, J.; Martinez, F.; Tomas, M. *J. Chem. Soc., Dalton Trans.* **1980**, 888.

(3) Uson, R.; Fornies, J.; Martinez, F.; Tomas, M.; Reoyo, I. *Organometallics* **1983**, *2*, 1386.

(4) Uson, R.; Fornies, J.; Tomas, M.; Cotton, F. A.; Falvello, L. R. *J. Am. Chem. Soc.* **1984**, *106*, 2482. Uson, R.; Fornies, J.; Menjon, B.; Cotton, F. A.; Falvello, L. R.; Tomas, M. *Inorg. Chem.* **1985**, *24*, 4651.

(5) Uson, R.; Fornies, J.; Tomas, M.; Casas, J. M.; Cotton, F. A.; Falvello, L. R. *Polyhedron* **1986**, *5*, 901. Uson, R.; Fornies, J.; Tomas, M.; Casas, J. M.; Cotton, F. A.; Falvello, L. R. *Inorg. Chem.* **1986**, *25*, 4519.

(6) Uson, R.; Fornies, J.; Tomas, M.; Menjon, B. *Organometallics* **1986**, *5*, 1581.

Table III. Crystal Data for the Precursor $(NBu_4)_2[Pt_2(\mu\text{-}Cl)_2(C_6F_5)_4]$ (a) and for $(NBu_4)[Pt_2AgCl_2(C_6F_5)_4OEt_2]$ (**1**) (b)

	a	b
formula	$Pt_2Cl_2F_{20}N_2C_{56}H_{72}$	$Pt_2AgCl_2F_{20}ONC_{44}H_{46}$
fw	1614.3	1553.8
space group	$P2_1/c$	$P2_1/n$
syst abs	$0k0$, $k \neq 2n$ $h0l$, $l \neq 2n$	$0k0$, $k \neq 2n$ $h0l$, $h + l \neq 2n$
a, Å	12.763 (4)	12.574 (2)
b, Å	12.858 (4)	14.749 (2)
c, Å	19.554 (7)	27.983 (3)
β, deg	104.62 (2)	92.73 (1)
V, Å^3	3105 (2)	5184 (2)
Z	2	4
d_{calcd}, g/cm^3	1.726	1.991
cryst size, mm	0.25 × 0.19 × 0.17	0.27 × 0.22 × 0.09
μ(Mo Kα), cm^{-1}	49.3	62.4
data collcn instrument	Syntex P$\bar{1}$	CAD-4
radiation (monochromated in incident beam)	Mo Kα ($\lambda_{\bar{\alpha}}$ = 0.71073 Å)	
orientation reflcns: no.; range (2θ), deg	15; $21 < 2\theta < 30°$	25; 19.9-30.6
temp, °C	3.5 ± 4.0	25 ± 3
scan method	ω–2θ	ω-scans
data collcn range (2θ), deg	4.0–50.0	4.0–50.0
no. of unique data; total no. with $F_o^2 > 3\sigma(F_o^2)$	3528; 2960	6358; 4252
no. of params refined	370	640
trans. factors; max, min	obsd 1.00, 0.39 calcd 0.43, 0.17	obsd 1.00, 0.80
R^a	0.0399	0.0397
$R_w{}^b$	0.0525	0.0448
quality-of-fit indicator^c	1.044	1.088
largest shift/esd, final cycle	0.03	0.02
largest peak, e/Å^3	0.67	0.71

[a] $R = \sum||F_o| - |F_c||/\sum|F_o|$. [b] $R_w = [\sum w(|F_o| - |F_c|)^2/\sum w|F_o|^2]^{1/2}$; $w = 1/\sigma^2(|F_o|)$. [c] Quality-of-fit $= [\sum w(|F_o| - |F_c|)^2/(N_{observn} - N_{params})]^{1/2}$.

Table IV. Positional Parameters and Equivalent Isotropic Displacement Parameters and Their Estimated Standard Deviations for $(NBu_4)_2[Pt_2(\mu\text{-}Cl)_2(C_6F_5)_4]$

atom	x	y	z	B^a, Å^2
Pt(1)	−0.12585 (3)	0.05152 (3)	0.00524 (2)	4.232 (8)
Cl(1)	−0.0064 (2)	0.0662 (3)	−0.0710 (2)	6.90 (7)
C(1)	−0.2246 (7)	0.1576 (8)	−0.0492 (5)	4.0 (2)
C(2)	−0.2878 (8)	0.1422 (8)	−0.1161 (5)	4.4 (2)
C(3)	−0.3524 (9)	0.219 (1)	−0.1560 (5)	5.3 (3)
C(4)	−0.3502 (9)	0.3175 (9)	−0.1283 (6)	5.5 (3)
C(5)	−0.2892 (9)	0.3380 (8)	−0.0631 (6)	5.1 (3)
C(6)	−0.2303 (8)	0.2566 (8)	−0.0255 (5)	4.6 (3)
C(7)	−0.2250 (8)	0.0289 (8)	0.0678 (5)	4.7 (2)
C(8)	−0.3209 (8)	−0.0250 (8)	0.0471 (5)	4.6 (3)
C(9)	−0.3895 (9)	−0.0436 (9)	0.0898 (6)	5.4 (3)
C(10)	−0.3662 (8)	−0.0054 (9)	0.1556 (5)	5.0 (2)
C(11)	−0.2723 (9)	0.0464 (9)	0.1803 (5)	4.9 (2)
C(12)	−0.2035 (8)	0.0637 (8)	0.1373 (5)	4.3 (2)
F(1)	−0.2935 (6)	0.0478 (5)	−0.1470 (4)	7.2 (2)
F(2)	−0.4139 (7)	0.1999 (7)	−0.2217 (4)	9.1 (2)
F(3)	−0.4097 (6)	0.3932 (6)	−0.1677 (4)	8.5 (2)
F(4)	−0.2896 (7)	0.4333 (5)	−0.0358 (5)	8.6 (2)
F(5)	−0.1717 (6)	0.2839 (5)	0.0406 (4)	7.2 (2)
F(6)	−0.3502 (6)	−0.0654 (5)	−0.0185 (4)	6.9 (2)
F(7)	−0.4816 (6)	−0.0984 (6)	0.0656 (4)	8.1 (2)
F(8)	−0.4327 (5)	−0.0209 (6)	0.1982 (4)	7.4 (2)
F(9)	−0.2453 (6)	0.0863 (6)	0.2472 (3)	7.4 (2)
F(10)	−0.1109 (5)	0.1160 (5)	0.1649 (3)	6.4 (2)
N(1)	0.2120 (7)	0.2754 (7)	0.1551 (5)	5.8 (2)
C(13)	0.1486 (9)	0.3523 (9)	0.1902 (6)	5.5 (3)
C(14)	0.040 (1)	0.308 (1)	0.1990 (7)	7.3 (4)
C(15)	−0.012 (1)	0.391 (1)	0.2376 (7)	7.6 (4)
C(16)	−0.126 (1)	0.352 (1)	0.2443 (8)	8.4 (4)
C(17)	0.3154 (9)	0.3353 (9)	0.1534 (7)	5.9 (3)
C(18)	0.397 (1)	0.273 (1)	0.1236 (7)	6.7 (3)
C(19)	0.4850 (9)	0.350 (1)	0.1114 (7)	6.5 (3)
C(20)	0.573 (1)	0.290 (1)	0.0870 (8)	8.1 (4)
C(21)	0.242 (1)	0.1772 (8)	0.2019 (7)	6.4 (3)
C(22)	0.297 (1)	0.202 (1)	0.2809 (7)	7.5 (4)
C(23)	0.317 (2)	0.098 (1)	0.3204 (9)	10.2 (5)
C(24)	0.369 (2)	0.121 (1)	0.3984 (9)	10.6 (5)
C(25)	0.145 (1)	0.238 (1)	0.0807 (8)	9.2 (5)
C(26)	0.106 (2)	0.334 (2)	0.0286 (8)	12.8 (7)
C(27)	0.079 (3)	0.311 (2)	−0.041 (1)	23 (1)
C(28)	0.042 (2)	0.389 (2)	−0.090 (1)	14.4 (8)

[a] B values for anisotropically refined atoms are given in the form of the isotropic equivalent thermal parameter defined as $^4/_3[a^2\beta_{11} + b^2\beta_{22} + c^2\beta_{33} + ab(\cos\gamma)\beta_{12} + ac(\cos\beta)\beta_{13} + bc(\cos\alpha)\beta_{23}]$.

Table V. Selected Bond Distances (Å) and Angles (deg) for $(NBu_4)_2[Pt_2(\mu\text{-}Cl)_2(C_6F_5)_4]^a$

	Distances		
Pt(1)–Cl(1)	2.394 (3)	C(1)–C(2)	1.367 (14)
Pt(1)–Cl(1′)	2.387 (3)	C(1)–C(6)	1.363 (14)
Pt(1)–C(1)	1.977 (10)	C(7)–C(8)	1.375 (15)
Pt(1)–C(7)	1.991 (10)	C(7)–C(12)	1.39 (2)
	Angles		
Cl(1)–Pt(1)–Cl(1′)	84.9 (1)	Pt(1)–C(1)–C(2)	123.9 (8)
Cl(1)–Pt(1)–C(1)	91.7 (3)	Pt(1)–C(1)–C(6)	122.8 (8)
Cl(1)–Pt(1)–C(7)	176.1 (3)	C(2)–C(1)–C(6)	113 (1)
Cl(1′)–Pt(1)–C(1)	174.9 (3)	Pt(1)–C(7)–C(8)	123.3 (9)
Cl(1′)–Pt(1)–C(7)	92.8 (3)	Pt(1)–C(7)–C(12)	123.7 (9)
C(1)–Pt(1)–C(7)	90.8 (4)	C(8)–C(7)–C(12)	113 (1)
Pt(1)–Cl(1)–Pt(1′)	95.1 (1)		

[a] Numbers in parentheses are estimated standard deviations in the least significant digits.

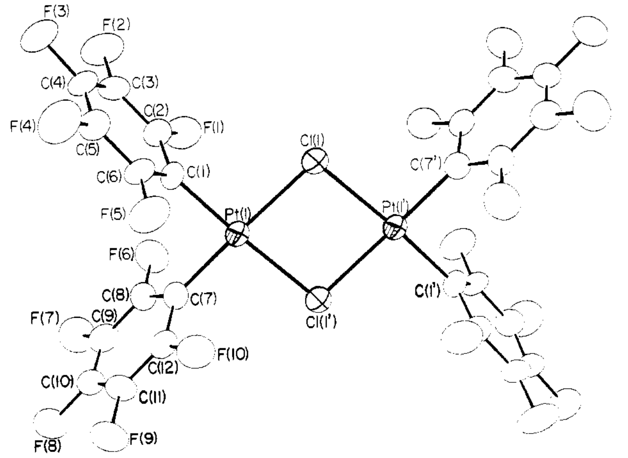

Figure 1. ORTEP plot of the dianion $[Pt_2(\mu\text{-}Cl)_2(C_6F_5)_4]^{2-}$. All atoms are represented by their 35% probability ellipsoids.

Analytical and conductance data are given in Table I. Relevant IR data for the products reported are gathered in Table II.

Structures. The structures both of the precursor $(NBu_4)_2[Pt_2(\mu\text{-}Cl)_2(C_6F_5)_4]$ and of complex **1**, $(NBu_4)[Pt_2Ag(\mu\text{-}Cl)_2(C_6F_5)_4O(C_2H_5)_2]$, have been determined by single-crystal X-ray diffraction. General crystallographic information is given in Table III.

$(NBu_4)_2[Pt_2(\mu\text{-}Cl)_2(C_6F_5)_4]$. Positional and equivalent isotropic displacement parameters are listed in Table IV, and selected bond distances and angles are given in Table V. Figure 1 shows the structure of the complex anion, which sits on a crystallographic inversion center. The core of the complex consists of two platinum atoms with a pair of chlorine bridges. Each Pt atom has two cis C_6F_5 groups in terminal positions, completing the usual planar four-coordination. The entire $Pt_2Cl_2C_4$ core of the dianion is planar. The two unique Pt–Cl distances (Pt(1)–Cl(1) = 2.394 (3) Å; Pt(1)–Cl(1′) = 2.387 (3) Å) are equal within experimental error, in line with their equivalent roles as bridging ligands trans to the same substituents. Similarly, the terminal Pt–C bond

Table VI. Table of Positional Parameters and Their Estimated Standard Deviations for $(NBu_4)[Pt_2AgCl_2(C_6F_5)_4OEt_2]$

atom	*x*	*y*	*z*	*B*,[a] Å^2	atom	*x*	*y*	*z*	*B*,[a] Å^2
Pt(1)	0.42808 (4)	0.20783 (4)	−0.10903 (2)	3.87 (1)	F(3)	0.7435 (7)	0.2057 (7)	−0.2703 (3)	9.6 (3)
Pt(2)	0.18066 (4)	0.14157 (4)	−0.10777 (2)	4.11 (1)	F(4)	0.5327 (9)	0.2268 (8)	−0.2912 (3)	10.7 (3)
Ag(1)	0.25103 (9)	0.30147 (7)	−0.14651 (4)	5.35 (3)	F(5)	0.3941 (7)	0.2301 (7)	−0.2222 (3)	7.6 (2)
Cl(1)	0.3025 (3)	0.2022 (3)	−0.0471 (1)	4.98 (8)	F(6)	0.4612 (6)	0.4073 (5)	−0.1524 (3)	6.4 (2)
Cl(2)	0.3381 (3)	0.0737 (2)	−0.1386 (1)	4.98 (8)	F(7)	0.5514 (8)	0.5543 (5)	−0.1123 (3)	8.1 (3)
O(1)	0.2088 (8)	0.4515 (6)	−0.1591 (3)	6.5 (3)	F(8)	0.6349 (7)	0.5503 (5)	−0.0216 (3)	7.4 (2)
C(1)	0.530 (1)	0.2098 (9)	−0.1601 (4)	4.4 (3)	F(9)	0.6259 (7)	0.3967 (6)	0.0301 (3)	6.6 (2)
C(2)	0.639 (1)	0.1997 (9)	−0.1529 (4)	4.9 (3)	F(10)	0.5412 (6)	0.2465 (5)	−0.0086 (3)	6.0 (2)
C(3)	0.709 (1)	0.198 (1)	−0.1886 (6)	6.6 (4)	F(11)	0.1440 (7)	0.1949 (5)	−0.2188 (3)	7.2 (2)
C(4)	0.674 (1)	0.210 (1)	−0.2351 (5)	6.3 (4)	F(12)	0.0126 (8)	0.1263 (7)	−0.2866 (3)	9.4 (3)
C(5)	0.566 (1)	0.219 (1)	−0.2462 (5)	6.4 (4)	F(13)	−0.1179 (7)	−0.0140 (8)	−0.2679 (3)	10.0 (3)
C(6)	0.498 (1)	0.221 (1)	−0.2086 (5)	5.7 (4)	F(14)	−0.1174 (8)	−0.0818 (7)	−0.1783 (4)	11.2 (3)
C(7)	0.497 (1)	0.3191 (8)	−0.0820 (4)	4.0 (3)	F(15)	0.0121 (7)	−0.0152 (6)	−0.1084 (3)	7.7 (2)
C(8)	0.503 (1)	0.3993 (9)	−0.1064 (5)	4.5 (3)	F(16)	0.0114 (6)	0.2904 (6)	−0.1449 (3)	7.1 (2)
C(9)	0.548 (1)	0.4752 (9)	−0.0871 (5)	5.5 (4)	F(17)	−0.1461 (9)	0.3704 (7)	−0.1013 (5)	11.9 (4)
C(10)	0.590 (1)	0.4752 (9)	−0.0414 (5)	5.4 (3)	F(18)	−0.1862 (8)	0.3297 (8)	−0.0104 (4)	12.3 (3)
C(11)	0.588 (1)	0.3977 (9)	−0.0156 (5)	4.8 (3)	F(19)	−0.0662 (8)	0.2019 (9)	0.0369 (3)	11.7 (4)
C(12)	0.541 (1)	0.3207 (9)	−0.0359 (5)	5.2 (3)	F(20)	0.0872 (7)	0.1166 (7)	−0.0073 (3)	8.6 (3)
C(13)	0.084 (1)	0.0935 (8)	−0.1595 (5)	4.5 (3)	N(1)	0.5979 (9)	−0.1434 (7)	−0.1187 (4)	4.8 (3)
C(14)	0.081 (1)	0.1239 (9)	−0.2068 (5)	5.1 (3)	C(29)	0.507 (1)	−0.2156 (9)	−0.1250 (5)	5.1 (3)
C(15)	0.015 (1)	0.090 (1)	−0.2428 (5)	5.8 (4)	C(30)	0.397 (1)	−0.174 (1)	−0.1303 (6)	6.4 (4)
C(16)	−0.053 (1)	0.020 (1)	−0.2333 (5)	6.7 (4)	C(31)	0.316 (1)	−0.247 (1)	−0.1345 (7)	9.2 (6)
C(17)	−0.050 (1)	−0.014 (1)	−0.1884 (5)	6.5 (4)	C(32)	0.203 (1)	−0.211 (1)	−0.1413 (6)	8.8 (5)
C(18)	0.015 (1)	0.021 (1)	−0.1525 (5)	6.0 (4)	C(33)	0.585 (1)	−0.096 (1)	−0.0708 (5)	6.0 (4)
C(19)	0.059 (1)	0.1984 (9)	−0.0790 (5)	5.1 (3)	C(34)	0.682 (1)	−0.038 (1)	−0.0552 (5)	6.5 (4)
C(20)	−0.007 (1)	0.264 (1)	−0.0994 (5)	5.9 (4)	C(35)	0.647 (1)	0.025 (1)	−0.0136 (6)	7.4 (5)
C(21)	−0.088 (1)	0.308 (1)	−0.0779 (6)	7.6 (5)	C(36)	0.743 (1)	0.081 (1)	0.0059 (6)	9.0 (5)
C(22)	−0.107 (1)	0.286 (1)	−0.0308 (6)	8.4 (5)	C(37)	0.593 (1)	−0.072 (1)	−0.1582 (5)	6.8 (4)
C(23)	−0.048 (1)	0.224 (1)	−0.0094 (5)	7.7 (5)	C(38)	0.590 (2)	−0.108 (1)	−0.2089 (5)	8.5 (5)
C(24)	0.031 (1)	0.179 (1)	−0.0316 (5)	5.7 (4)	C(39)	0.591 (2)	−0.024 (1)	−0.2410 (6)	10.5 (6)
C(25)	0.234 (2)	0.500 (1)	−0.2015 (6)	9.3 (5)	C(40)	0.595 (2)	−0.042 (2)	−0.2914 (7)	13.1 (8)
C(26)	0.246 (2)	0.430 (1)	−0.2393 (6)	9.4 (6)	C(41)	0.707 (1)	−0.194 (1)	−0.1215 (5)	5.9 (4)
C(27)	0.200 (2)	0.511 (1)	−0.1171 (6)	9.0 (5)	C(42)	0.730 (1)	−0.264 (1)	−0.0824 (5)	6.6 (4)
C(28)	0.173 (2)	0.458 (1)	−0.0748 (5)	9.0 (5)	C(43)	0.839 (1)	−0.304 (1)	−0.0930 (7)	10.0 (6)
F(1)	0.6768 (6)	0.1875 (6)	−0.1078 (3)	6.9 (2)	C(44)	0.874 (2)	−0.378 (1)	−0.0618 (9)	11.8 (7)
F(2)	0.8137 (7)	0.1860 (7)	−0.1774 (3)	9.4 (3)					

[a] *B* values for anisotropically refined atoms are given in the form of the equivalent isotropic displacement parameter defined as $^4/_3[a^2\beta_{11} + b^2\beta_{22} + c^2\beta_{33} + ab(\cos\gamma)\beta_{12} + ac(\cos\beta)\beta_{13} + bc(\cos\alpha)\beta_{23}]$.

distances are roughly equivalent (Pt(1)–C(1) = 1.977 (10) Å; Pt(1)–C(7) = 1.991 (10) Å) and are in the range commonly found for Pt(II) complexes.[7,8] The bond angles around each Pt center are in the range 85–95°; the most acute angle is subtended by the two bridging chlorine atoms (Cl(1)–Pt(1)–Cl(1′) = 84.9 (1)°). The angle Pt(1)–Cl(1)–Pt(1′) has a value of 95.1 (1)°. The distance between the two platinum atoms is 3.528 (1) Å; thus, there is no electronic interaction between the two metal centers.

$(NBu_4)[Pt_2Ag(\mu\text{-}Cl)_2(C_6F_5)_4O(C_2H_5)_2]$ (1). Positional parameters and selected geometrical parameters are given in Tables VI and VII, respectively. The structure of the complex anion in **1** is shown in Figure 2. The core of the complex comprises two platinum atoms, 3.263 (1) Å apart, bridged by a single silver atom and two chlorine atoms. Each platinum center also has two terminal cis C_6F_5 groups, which complete a distorted square pyramid of five atoms about it. The two square pyramids share a pyramidal face, which is bounded by the two chlorine bridges and the silver atom. The two Pt–Ag distances differ slightly (Pt(1)–Ag(1) = 2.782 (1) Å; Pt(2)–Ag(1) = 2.759 (1) Å). Otherwise, the environments about the two platinum centers are similar to each other, and the Pt–Cl(bridging) and Pt–C (terminal) distances lie within the ranges expected for these structural types (see Table VII). We consider the distance between the two Pt atoms to indicate the absence of bonding between them, although Pt–Pt interactions have been invoked for systems in which the internuclear separations are greater (e.g., the 3.39-Å stacking separation in $[PtCl_4(en)]_4$[9]). The silver atom is three-coordinate, surrounded by the two platinum atoms and one diethyl ether molecule. The Ag–O distance is 2.299 (10) Å.

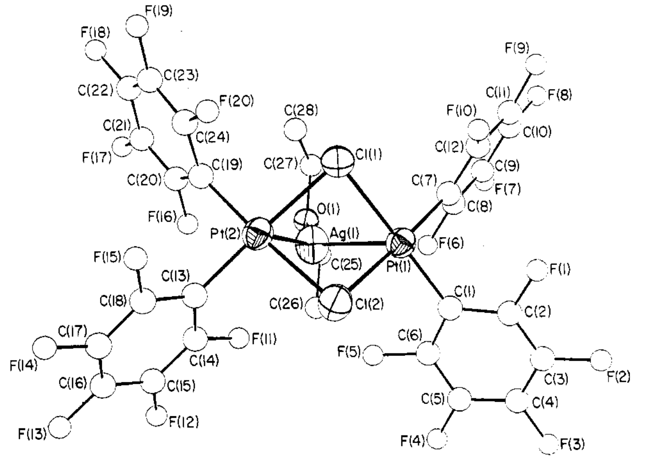

Figure 2. ORTEP drawing of the complex anion $[Pt_2AgCl_2(C_6F_5)_4OEt_2]^-$ from the crystal structure of **1**. Carbon and fluorine atoms are given as small circles, for clarity. The other atoms are represented by their 50% probability ellipsoids.

The short Pt–Ag distances and the absence of bridges on the Pt–Ag edges in **1** imply not only the presence of significant Pt–Ag bonding but also that these bonds are stronger than those in the previously reported C_6F_5-bridged derivative[1] $[Pt_2Ag(C_6F_5)_6]^-$. The Pt–Ag distances in the latter complex are 2.827 (2) and 2.815 (2) Å, and the overall stability of that complex is enhanced by the presence of short Ag···F contacts (2.66 and 2.67 Å) between the Ag center and *o*-F atoms of the bridging C_6F_5 ligands. Complex **1**, which has chlorine bridges in place of C_6F_5, cannot benefit from such close contacts—the shortest Ag···F distance in **1** is 2.84 Å. The electrophilicity of the Ag center in **1** is satisfied

---

(7) Watkins, S. F. *J. Chem. Soc. A.* **1970**, 168.
(8) Whitla, W. A.; Powell, H. M.; Venanzi, L. M. *J. Chem. Soc., Chem. Commun.* **1966**, 310.
(9) Martin, D. S., Jr.; Jacobson, R. A.; Hunter, L. D.; Benson, J. E. *Inorg. Chem.* **1970**, *9*, 1276.

Table VII. Selected Distances (Å) and Angles (deg) for $(NBu_4)[Pt_2AgCl_2(C_6F_5)_4]$[a]

Distances			
Pt(1)···Pt(2)	3.263 (1)	Ag(1)–O(1)	2.299 (10)
Pt(1)–Ag(1)	2.782 (1)	O(1)–C(25)	1.43 (2)
Pt(1)–Cl(1)	2.401 (3)	O(1)–C(27)	1.48 (2)
Pt(1)–Cl(2)	2.406 (3)	C(1)–C(2)	1.39 (2)
Pt(1)–C(1)	1.960 (13)	C(1)–C(6)	1.41 (2)
Pt(1)–C(7)	1.987 (13)	C(7)–C(8)	1.37 (2)
Pt(2)–Ag(1)	2.759 (1)	C(7)–C(12)	1.38 (2)
Pt(2)–Cl(1)	2.404 (3)	C(13)–C(14)	1.40 (2)
Pt(2)–Cl(2)	2.414 (3)	C(13)–C(18)	1.40 (2)
Pt(2)–C(13)	1.975 (13)	C(19)–C(20)	1.37 (2)
Pt(2)–C(19)	1.956 (15)	C(19)–C(24)	1.42 (2)
Angles			
Ag(1)–Pt(1)–Cl(1)	75.36 (9)	Pt(1)–Ag(1)–Pt(2)	72.15 (3)
Ag(1)–Pt(1)–Cl(2)	85.62 (9)	Pt(1)–Ag(1)–O(1)	135.3 (3)
Ag(1)–Pt(1)–C(1)	104.8 (4)	Pt(2)–Ag(1)–O(1)	143.8 (3)
Ag(1)–Pt(1)–C(7)	93.4 (4)	Pt(1)–Cl(1)–Pt(2)	85.5 (1)
Cl(1)–Pt(1)–Cl(2)	84.5 (1)	Pt(1)–Cl(2)–Pt(2)	85.2 (1)
Cl(1)–Pt(1)–C(1)	178.7 (4)	Ag(1)–O(1)–C(25)	123 (1)
Cl(1)–Pt(1)–C(7)	92.4 (4)	Ag(1)–O(1)–C(27)	118.6 (9)
Cl(2)–Pt(1)–C(1)	94.2 (4)	C(25)–O(1)–C(27)	113 (1)
Cl(2)–Pt(1)–C(7)	176.9 (4)	Pt(1)–C(1)–C(2)	125 (1)
C(1)–Pt(1)–C(7)	88.8 (5)	Pt(1)–C(1)–C(6)	123 (1)
Ag(1)–Pt(2)–Cl(1)	75.77 (9)	C(2)–C(1)–C(6)	113 (1)
Ag(1)–Pt(2)–Cl(2)	86.00 (8)	Pt(1)–C(7)–C(8)	124 (1)
Ag(1)–Pt(2)–C(13)	102.5 (4)	Pt(1)–C(7)–C(12)	121 (1)
Ag(1)–Pt(2)–C(19)	93.9 (4)	C(8)–C(7)–C(12)	115 (1)
Cl(1)–Pt(2)–Cl(2)	84.3 (1)	Pt(2)–C(13)–C(14)	125 (1)
Cl(1)–Pt(2)–C(13)	177.8 (4)	Pt(2)–C(13)–C(18)	122 (1)
Cl(1)–Pt(2)–C(19)	92.1 (4)	C(14)–C(13)–C(18)	113 (1)
Cl(2)–Pt(2)–C(13)	94.3 (4)	Pt(2)–C(19)–C(20)	127 (1)
Cl(2)–Pt(2)–C(19)	176.3 (4)	Pt(2)–C(19)–C(24)	122 (1)
C(13)–Pt(2)–C(19)	89.3 (5)	C(20)–C(19)–C(24)	111 (1)

[a] Numbers in parentheses are estimated standard deviations in the least significant digits.

by stronger bonds to the Pt atoms.

A comparison of the two structures reported here shows that two major structural modifications occur upon reaction of Ag^+ with the planar core of the precursor $[Pt_2(\mu\text{-}Cl)_2(C_6F_5)_4]^{2-}$. First, the planar Pt_2Cl_2 core of the precursor folds in such a way that in the product, **1**, the planes Pt(1), Cl(1), Cl(2) and Pt(2), Cl(1), Cl(2) form a dihedral angle of 47.5 (1)°. The two chlorine atoms are displaced away from the silver center, which receives electron density only from the Pt atoms. Secondly, the angles subtended at the chlorine bridges, which have a common value of 95.1 (1)° in the precursor, are about 10° more acute (85.5 (1) and 85.2 (1)°) in complex **1**. As with the folding of the core, this effect coincides with the increased stress on the precursor fragment, caused by the incorporation of a third bridge.

IR Spectra. Table II lists significant IR absorption frequencies for complexes **1**–**4**, all of which give internal bands of the C_6F_5 groups located at 1500 (s), 1260 (s), 1050 (s), and 955 (s) cm^{-1}. Moreover, the X-sensitive modes of this group appear as a double band (Table II) confirming the cis disposition of two C_6F_5 groups around each Pt atom.[10] The chlorocomplexes **1**, **3**, **4** show a broad absorption at 260 cm^{-1}, due to ν(Pt–Cl) shifted to lower energies relative to the precursor (290 cm^{-1}).[2]

Experimental Section

C, H, and N analyses and conductance measurements were performed as described elsewhere.[2] IR spectra (4000–200 cm^{-1}) were recorded on a Perkin-Elmer 599 spectrophotometer by using Nujol mulls between polyethylene sheets. $(NBu_4)_2[Pt_2(\mu\text{-}X)_2(C_6F_5)_4]$ was prepared as described elsewhere.[2] All the reactions were carried out under exclusion of light.

Preparation of $(NBu_4)[Pt_2AgX_2(C_6F_5)_4OEt_2]$ (X = Cl (1), Br (2)). To a solution of $(NBu_4)_2[Pt_2(\mu\text{-}X)_2(C_6F_5)_4]$ (X = Cl, 0.2 g, 0.1 mmol; X = Br, 0.31 g, 0.18 mmol) in 20 mL of CH_2Cl_2 was added an equimolar amount of $AgClO_4$, and the mixture was stirred at room temperature for 3 h. No AgX precipitation was observed. The solution was evaporated to dryness, and the resulting oily residue was treated with 25 mL of $(C_2H_5)_2O$ to separate the insoluble NBu_4ClO_4. The ether solution was evaporated to dryness, and the white residue was washed with 10 mL of *n*-hexane. Complexes **1** and **2** were isolated in 88% and 77% yields, respectively.

Preparation of $(NBu_4)[Pt_2AgCl_2(C_6F_5)_4L]$ (L = PPh_3 (3), $PMePh_2$ (4)). A typical preparation was as follows: To a solution of 0.2 g (0.1 mmol) of $(NBu_4)_2[Pt_2(\mu\text{-}Cl)_2(C_6F_5)_4]$ in 10 mL of CH_2Cl_2 at −30 °C was added 0.582 g (0.124 mmol) of $AgOClO_3PPh_3$, and the mixture was stirred for 30 min at this temperature. The solution was pumped to dryness (−30 °C), and the resulting oily residue was treated with 20 mL of $(C_2H_5)_2O$ (−30 °C). After separation of the insoluble NBu_4ClO_4, the solution was evaporated almost to dryness and 10 mL of *n*-hexane was added. A pale-yellow solid (complex **3**, 83% yield) was obtained.

Under similar conditions complex **4** can be obtained. Reagents: 0.20 g (0.124 mmol) of $(NBu_4)_2[Pt_2(\mu\text{-}Cl)_2(C_6F_5)_4]$; 0.0504 g (0.124 mmol) of $AgOClO_3PMePh_2$ in CH_2Cl_2. Yield: 45%.

Reaction of $(NBu_4)[Pt_2AgCl_2(C_6F_5)_4OEt_2]$ (1) with PPh_3. To a solution of 0.1 g (0.0644 mmol) of complex **1** in 10 mL of CH_2Cl_2 at −30 °C, was added 0.0169 g (0.0644 mmol) of PPh_3, and the mixture was stirred for 15 min. The solution was evaporated to dryness at −30 °C and the oily yellow residue was washed with 10 mL of *n*-hexane (−30 °C). By addition of CH_2Cl_2/*n*-hexane (2/10 mL) (−30 °C) and evaporation to ~5 mL, complex **3** (60% yield) was obtained.

Preparation of Crystals for X-ray Structure Determination. Crystals of $(NBu_4)_2[Pt_2(\mu\text{-}Cl)_2(C_6F_5)_4]$ and of $(NBu_4)[Pt_2AgCl_2(C_6F_5)_4OEt_2]$ (**1**) were obtained by slow diffusion at −30 °C of *n*-hexane into dichloromethane solutions of the corresponding complexes.

Crystal Structure Analyses. The relevant crystal data and structure analysis parameters are summarized in Table III for the structure determinations of the precursor $(NBu_4)_2[Pt_2Cl_2(C_6F_5)_4]$ and of product **1**, $(NBu_4)[Pt_2AgCl_2(C_6F_5)_4OEt_2]$. In each case, a single crystal was mounted at the end of a glass fiber and covered with a thin layer of epoxy. Procedures that have been previously described[11] were used for data collection and processing. An empirical absorption correction[12] based on azimuthal scans was applied in each case. In the case of $(NBu_4)_2[Pt_2Cl_2(C_6F_5)_4]$, three monitor reflections lost an average of 6.4% of their initial intensities during the course of 148 h of X-ray exposure. For **1**, three check reflections lost an average of 10.9% of their initial intensities during 149 h of X-ray exposure. Decay corrections were applied to both data sets.

The structure of the precursor was solved by direct methods and developed via difference Fourier maps. After isotropic convergence, a further absorption correction was applied by the method of Walker and Stuart.[13] In the final refinement, all 41 unique atoms were anisotropic.

The structure of **1** was solved by interpretation of the Patterson map; it was developed and refined in an alternating sequence of least-squares cycles and difference Fourier maps. In the final refinement, all 71 atoms had anisotropic displacement parameters. A difference map following the last refinement showed several ghost peaks near the platinum atoms; however, there were no chemically significant difference peaks.

Acknowledgment. We thank the National Science Foundation and the CAYCIT (Spain) for financial support.

Supplementary Material Available: For both crystal structures, full tables of bond distances, bond angles, and anisotropic displacement parameters (10 pages); lists of observed and calculated structure factors for both crystal structures (37 pages). Ordering information is given on any current masthead page.

---

(10) Maslowsky, E., Jr. *Vibrational Spectra of Organometallic Compounds*; Wiley: New York, 1977; p 437 and references given therein.

(11) (a) Syntex P$\bar{1}$: Cotton, F. A.; Frenz, B. A.; Deganello, G.; Shaver, A. *J. Organomet. Chem.* **1973**, *50*, 227. (b) CAD-4F: Bino, A.; Cotton, F. A.; Fanwick, P. E. *Inorg. Chem.* **1979**, *18*, 3558.

(12) North, A. C. T.; Phillips, D. C.; Mathews, F. S. *Acta Crystallogr., Sect. A: Cryst. Phys., Diffr., Theor. Crystallogr.* **1968**, *24*, 351.

(13) Walker, N.; Stuart, D. *Acta Crystallogr., Sect. A: Found. Crystallogr.* **1983**, *39*, 158.